

Mercury capture on coal combustion fly ash

David J. Hassett*, Kurt E. Eylands

Energy and Environmental Research Center, University of North Dakota, PO Box 9018, Grand Forks, ND 58202-9018, USA

Received 5 January 1998; received in revised form 7 July 1998

Abstract

A study was performed at the Energy and Environmental Research Center (EERC) to test the hypotheses that (1) different carbon types contained in coal combustion fly ash have variable sorption capabilities relative to mercury and (2) the inorganic fraction of coal combustion fly ash may sorb mercury through mechanisms distinct from sorption by carbon in the ash. The purpose of this study was to conduct laboratory experiments to better understand the phenomenon of mercury sorption on coal combustion fly ash. Tests were conducted on the laboratory scale using samples generated from both commercial-scale utility boilers and pilot-scale combustion equipment at the EERC. Selected samples represented ash from various coal sources, of varying loss-on-ignition (LOI) content, and exhibiting different combinations of carbon types. Results indicate a direct correlation between carbon content and mercury partitioning among individual ash samples. The direct relationship between carbon content and mercury-sorbing capacity of the bulk ash samples demonstrated in the loading experiments is not reflected by the low- and high-carbon fraction data. The mercury-sorbing capacity of the inorganic fraction is extremely low with respect to carbon present in the ash. There are likely to be significant differences between the mercury-sorbing capacities of these various carbon forms. The mercury-sorbing capacity of ash studied in this research was highly temperature dependent. Additional work is needed on experimental design to evaluate the loading of high-carbon ash samples with particular attention to the phenomenon of sorptive capacity regeneration, which should be further investigated. Published by Elsevier Science Ltd.

Keywords: Mercury; Fly ash; Carbon; Sorption

1. Introduction

Mercury capture on fly ash has been attributed to the carbon contained in fly ash, but the capture efficiency noted in our studies does not directly correlate with the LOI values [1, 2]. Loss on ignition is commonly used as an indicator of carbon content in fly ash, although other attributes of the fly ash may also contribute to the LOI value. Carbon is thought to play a significant role in mercury capture on fly ash, but other mechanisms or factors related to carbon types may also contribute to this capture. A study was performed at the Energy and Environmental Research Center (EERC) to test the following hypotheses:

1. Different carbon types contained in coal combustion fly ash have different mercury sorption capabilities.
2. The inorganic fraction of coal combustion fly ash may sorb mercury through mechanisms distinct from sorption by carbon in the ash.

2. Experimental

2.1. Mercury sorption apparatus

A continuous cold-vapor mercury generation assembly from a Leeman PS200 automated mercury analyzer was used to generate mercury vapor at known concentrations. The gas–liquid separator was used as supplied by the manufacturer and run according to instrument specifications. Reagents were fed to the gas–liquid separator using a variable-speed peristaltic pump so that the concentration of mercury vapor could be continuously varied as required. Mercury vapor from the vapor generation apparatus was continuously monitored using a Brooks Rand CVAFS-2 atomic fluorescence mercury analyzer.

2.2. Design of sorption experiments

The sorption experiments were designed both as a preliminary screening procedure to aid sample selection and to fully load selected samples with mercury and achieve breakthrough, which would determine maximum loading of each sample. Mercury vapor was generated by mixing solutions

* Corresponding author. Tel.: + 1-701-777-5192; Fax: + 1-701-777-5181; e-mail: dhassett@eerc.und.nodak.edu.

Table 1
Coal combustion fly ash samples subjected to screening procedure

Sample ID	Sample description	Loss on ignition (wt%)	Results of screening procedure. Sorbed mercury: Yes or No
Blank	Quartz	NA	N (35 s to breakthrough)
Pilot-scale samples			
Lignite 1 (Falkirk)	Gray	1.03	Y (75 min to breakthrough)
Lignite 2 (Absaloka)	Light gray	0.41	Y (10 min to breakthrough)
Subbituminous 1 (Comanche)	Tan	0.02	N
Bituminous 1 (Blacksville)	Black	9.70	Y (breakthrough not achieved in screening)
Commercial-scale samples			
Lignite 3	Light tan	0.02	N
Bituminous 2	Dark gray	9.92	Y (breakthrough not achieved in screening)
Bituminous 3	Dark gray	4.79	Y (breakthrough not achieved in screening)

of 500 ng/ml mercury and 10 wt% stannous chloride, both in 10% hydrochloric acid, in the gas–liquid separator cell at nominal rates of 0.6 and 0.12 ml/min, respectively, using a variable-speed peristaltic pump. Gas flow through the gas–liquid separator/stripping cell was held at 150 ml/min. This resulted in a mercury concentration of 2 µg of mercury per l of argon gas. A sidestream of 20–30 ml/min was taken from the stripping cell with an additional pump and used to saturate the ash samples selected for study.

The concentration of mercury used for saturation of samples was considerably higher than would be found at a typical coal-burning power generation station. A relatively high concentration was used to expedite saturation of samples and was not intended to be a simulation of power plant conditions. Simulation of power plant sorption phenomena would have required not only lower concentrations of mercury, but also the use of simulated flue gas with all of the associated gaseous components. These experiments carried out in argon gas were intended to provide preliminary data for an ongoing research effort.

2.3. Sample screening and selection

A large number of coal combustion fly ash samples was screened using the mercury sorption apparatus (listed in Table 1). Sample selection criteria were (1) select samples representative of the three major coal types used in the USA, (2) compare pilot- and commercial-scale samples where available, and (3) select samples exhibiting a range of loss-on-ignition (LOI) values. Initially, a short-duration sorption test was performed on each sample to determine the amount of sample that would optimize the gas flow through the sample chamber and which samples actually acted as mercury sorbents. Samples included those available from the EERC's particulate test combustor (PTC) and from industry sources. Operating parameters and extensive characterization information were available for the EERC samples generated on the pilot scale; however, for the samples submitted by industry, information was limited to coal type and LOI.

Samples of ash were packed into 10 mm glass tubes for sorption experiments. Initially, approximately 600 mg of ash was placed into each tube; however, high-carbon ash samples were reduced from 600 mg to between 100 and 150 mg after it was observed that extremely long durations (up to weeks) would be required to saturate the larger quantity. As noted, an atomic fluorescence detector was used to monitor the gas stream from the ash tubes being saturated. Each sample was subjected to the mercury vapor flow either until breakthrough was achieved or for a maximum of 8 h. Some of the ash samples had a high mercury sorption capacity, and it was estimated that days or weeks might be required to achieve saturation and breakthrough. The samples were those exhibiting higher LOI. Based upon observation during the screening experiments, it was decided to eliminate breakthrough curves during the screening, as the development of breakthrough curves was impractical. The screening procedure results are given in Table 1.

The results of the screening experiments indicated that the high LOI samples (> 2 wt%) were the most efficient mercury sorbers. The samples with moderate LOI values (between 0.05 and 2 wt% LOI) sorbed mercury, but breakthrough was achieved in a short time. The only two samples identified as nonsorbers had very low LOI values (both 0.02 wt% LOI). If it is assumed that LOI is a good approximation of carbon content, these results are consistent with the assumption that carbon in ash is primarily responsible for mercury sorption. These results provided baseline information for sample selection to evaluate the stated hypotheses.

Samples selected for detailed sorption experiments and further characterization included Lignite 1, Lignite 3, Subbituminous 1, Bituminous 1, and Bituminous 2 (see Table 1). These samples met all selection criteria with the exception of providing information for comparison of pilot- and commercial-scale samples for subbituminous coal. No sample of commercial-scale subbituminous coal fly ash was available for this study.

Table 2
Ash/carbon separation (%mass)

Position on electrode	Bituminous 1	Lignite 1
Pa (low-C fraction)	9.61	6.81
Pb	16.07	8.39
Pc	13.37	7.65
Pd	9.49	7.14
Na (high-C fraction)	3.59	7.86
Nb	7.16	10.98
Nc	7.18	8.57
Nd	6.28	7.39
Downstream filter	14.67	12.16
Total loss	12.58	23.05

3. Results

3.1. Sample separation

To test the hypothesis, it was necessary to separate the inorganic and carbon fractions of the samples. Limitations of both commercial- and laboratory-scale separation techniques do not allow complete separation of the carbon and inorganic fractions of samples such as fly ash, so the sample fractions are more appropriately labeled ‘high C’ and ‘low C’. The original samples are labeled ‘bulk’ throughout the remainder of the text.

Several of the commercial-scale samples had been separated at the utility site, so the high- and low-carbon fractions were already available. The commercial-scale operation technique used electrostatic separation on a horizontal moving belt. Only one of the selected commercial-scale samples and all of the samples generated in the EERC pilot-scale combustion tests required separation. The two samples requiring separation with the highest LOI values (Lignite 1 and Bituminous 1) were submitted to the University of Kentucky (UK) Center for Applied Energy Research to be separated by a laboratory-scale electrostatic separation system. The remaining samples had LOI values of $< 1\%$, and the effectiveness of the separation technique for samples of that type had not been demonstrated. Separation results for the Lignite 1 (LOI = 1.03 wt%) indicated poor efficiency. Mercury sorption experiments were completed on the bulk samples only.

The UK Center for Applied Energy Research uses a type of electrostatic separation process in which samples are collected from the top, center, and bottom of both positive and negative electrodes. A filter was set up downstream to collect those particles not charge-separated. Each sample was separated into nine fractions, and the mass percent of each fraction was reported, as well as total loss based on mass balance. Table 2 shows the results as received from UK.

Each fraction represents a position on the electrode from which it was collected. The Pa sample was collected from the top of the positive electrode, and Pd was collected from the bottom of the positive electrode. Similarly, Na is from

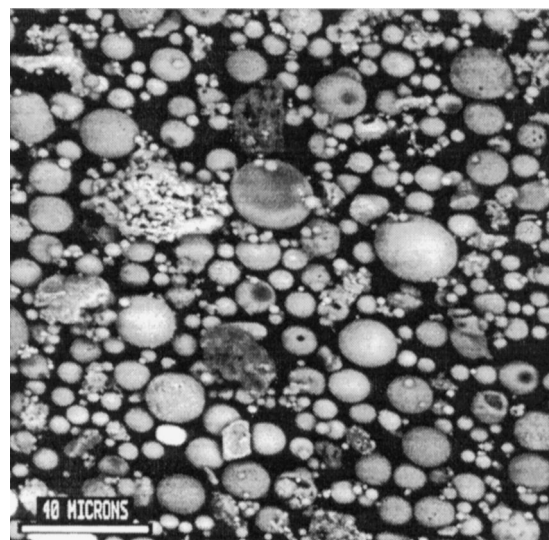


Fig. 1. Backscattered SEM image of the lignite char from the top of the negative electrode.

the top of the negative electrode and Nd from the bottom. The fractions designated as Pa by UK were selected as the low-C fraction and those designated Na as the high-C fraction.

3.2. Carbon characterization

Carbon in bulk samples and in high- and low-C fractions was evaluated by (1) total carbon content and (2) carbon type or morphology. High-C fractions from two commercial-scale power plants and two PTC tests were selected for carbon characterization.

In all of the samples examined, a majority (approximately 80–90%) of the carbon fraction was composed of very fine flakes and needles too small to identify size and morphology with a reflected light binocular microscope. In the high-C samples, three types of the larger carbon particles were most commonly observed, making up a very small portion of the total carbon fraction. These morphotypes generally varied in the number of vesicles (bubbles, which affects their appearance). Those particles with few vesicles appear smooth and have a higher luster, whereas a highly vesiculated particle has a dull appearance and is very friable, contributing to the very fine portion. There were also a few, rare carbon grains that showed very little alteration from combustion. These grains are usually blocky and have visible striations preserving the original woody texture of the carbon.

3.2.1. Lignite 1 high-C fraction

The lignite char sample from the PTC contained very little carbon as received (0.9%). When separation of the carbon and ash was attempted at UK, the fractions of the sample that should have contained the greatest amount of carbon were found to contain very little. Fig. 1 is a back-scattered electron image from a Noran Instruments ADEM

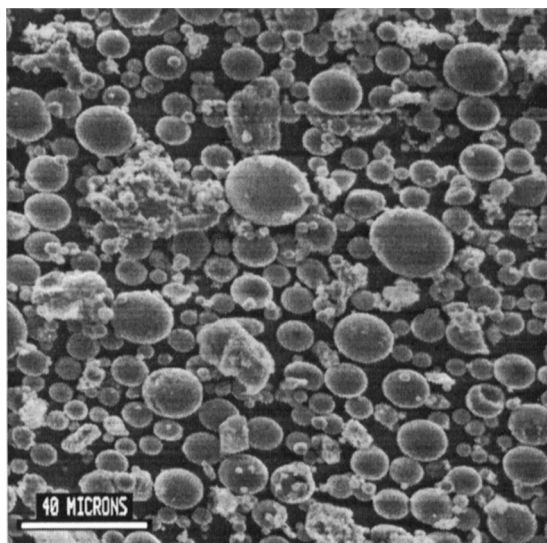


Fig. 2. Secondary SEM image of the lignite char sample from the top of the negative electrode.

scanning electron microscope (SEM) of a representative view of the lignite char sample. A backscattered image indicates atomic number differences by showing compounds having a higher atomic number as a lighter gray than a compound of a lower atomic number. Fig. 1 shows few actual char particles (dark gray), while most of the sample is fly ash. The few carbon particles visible in Fig. 1 have a blocky appearance with no rounding because swelling and vesiculation are minimal. Fig. 2 is a secondary SEM image of the same area as Fig. 1. The overall particle size is larger than the bituminous char in Fig. 3 and Fig. 4 partially as a result of the lesser amount of friable carbon.



Fig. 3. Backscattered image of the bituminous char taken from the top of the negative electrode.

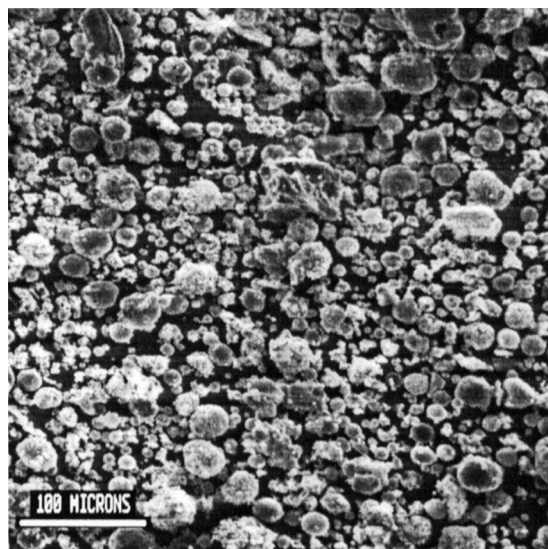


Fig. 4. Secondary SEM image of the bituminous char from the top of the negative electrode.

3.2.2. Bituminous 1 high-C fraction

The bituminous ash had an original carbon content of 8.4% as shown by C–H–N analysis. The top of the negative electrode (Na) sample, the darkest of the nine fractions, was selected for visual examination based on the amount of carbon. Although the maximum size of the char particles examined was about 50 μm (0.05 mm), the particle morphology of the char was very similar to that of bituminous chars from the full-scale samples. The swollen, high-luster particles with little vesiculation were the dominant type, followed by the highly vesiculated types. Carbon particle size is fairly variable, but here most of the extremely fine material is the result of the mechanical breakdown of the more vesiculated particles, which are more brittle and can have extremely thin walls.

Fig. 3 is a backscattered electron image of a representative view of the bituminous char sample. The carbon particles in Fig. 3 are the darkest gray, with the black representing the spaces in between the particles. The white particles are mostly fly ash spheres of inorganic compounds. The various gray levels mostly represent varying amounts of inorganic material contained in the char. These range from a few extremely small spheres on the surface of the carbon to nearly completely fused agglomerations as the carbon was combusting.

Fig. 4 is a secondary image of the same area shown in the backscattered image in Fig. 3 representing a typical view of the particles. There is generally a greater amount of the swollen, lightly vesiculated particles than the highly vesiculated particles as compared to the full-scale samples. The Bituminous 1 sample contained a significant amount of very fine carbon flakes and was generally finer-grained than other samples.

Table 3
Comparison of LOI and carbon content

Sample	LOI (wt%)	Carbon content (wt%)
Bituminous 3, high-C	60.40	48.50
Bituminous 2, high-C	27.65	26.94
Bituminous 2, bulk	9.92	8.94
Bituminous 1, bulk	9.70	8.36
Bituminous 3, bulk	4.79	4.09
Bituminous 2, low-C	1.43	1.02
Lignite 1	1.03	0.84
Bituminous 3, low-C	0.55	0.2

3.2.3. Comparison of LOI and carbon

LOI and carbon content have often been used interchangeably for evaluating ash. While the amount of carbon is likely to be the leading contributor to the LOI and there is a good correlation between LOI and high carbon, the two are different. Other compounds such as H_2O , $(\text{OH})^-$, and CO_3 all contribute to the LOI, which is simply the difference in weight after the material has been heated to 750°C for several hours. Ash that has aged and has been exposed to water will form several different inorganic compounds that include water as part of the crystalline structure. An example of this is the mineral ettringite, which forms as a hydration product in certain high-calcium ashes. Ettringite contains nearly 45% water by weight, which can be released during heating. Other Si and Al hydrates also form as a result of hydration. At the same time, not all of the carbon necessarily combusts during the LOI procedure. Carbon may develop structure (turbostratic carbon) that decreases its ability to combust. Graphitization of carbon carryover will still show up as carbon in a carbon analysis, but will not show up as LOI. Table 3 is a direct comparison of the LOI and carbon content for those samples in which both parameters were measured.

3.2.4. Mercury sorption experiments

The final mercury sorption experiments were performed using the protocol described above. Each of the bulk samples and the associated high- and low-C fractions were subjected to mercury vapor using the mercury sorption apparatus. Pre- and postloading samples of all bulk samples and fractions were submitted for total mercury analysis (Table 4). For ease of interpretation, LOI, carbon content, and sample color are also included in the table. A calculation indicating the mercury content with respect to only carbon has also been included.

Samples were exposed to mercury vapor until full mercury loading had been achieved (indicated by monitoring of input and output mercury concentrations). Total saturation of ash with mercury vapor was the goal in these experiments to allow comparisons to be made between ash samples. Total saturation was not considered indicative of the total capacity of ash for mercury under all conditions. Breakthrough indicates only that a gradient of concentration increase from the front of the ash sample to the back has progressed to the point where mercury vapor is detectable in the output gas stream. Thus, interpretation of data is difficult since different sorption phenomena may be responsible for the removal of mercury as the capacity of the ash becomes exhausted. Determination of bulk capacity for mercury removal was chosen as the approach for these experiments.

Several important observations were made during these final mercury sorption experiments. Despite the extended times allowed for high-C samples and fractions, it was still not feasible to achieve full mercury loading and breakthrough on some samples. As with the screening experiments, it was decided to eliminate the development of breakthrough data in the interest of time and budget. Additionally, during these experiments, it was noted that when the apparatus was turned off overnight, the high-C ash samples and fractions appeared to regenerate a portion of their sorptive capacity. Thus at the beginning of a second or third day, the

Table 4
Pre- and postloading mercury content of select samples

Sample ID	Sample description	LOI (wt%)	Carbon content (wt%)	Preloading mercury content ($\mu\text{g/g}$)	Preloading carbon content (mg/g)	Postloading carbon content (mg/g)	Postloading mercury content ($\mu\text{g/g}$)
Lignite 1, bulk	Gray	1.03	0.84	0.60	0.071	16	133
Lignite 1, low-C	Light gray	NA ^a	0.16	0.14	0.088	6.6	10.5
Lignite 1, high-C	Gray	NA	0.66	0.49	0.074	10.9	71.7
Subbituminous 1, bulk	Tan	0.19	NA	0.02			0.044
Bituminous 1, bulk	Black	9.70	8.36	0.36	0.004	0.08	6.92
Bituminous 1, low-C	Black	NA	1.22	0.11	0.009	2.0	24.1
Bituminous 1, high-C	Dark black	NA	33.96	2.41	0.007	14.3	4870
Lignite 3, bulk	Light tan	0.09	NA	0.02			0.63
Bituminous 2, bulk	Dark gray	9.92	8.94	0.17	0.002		NA
Bituminous 2, low-C	Gray	1.43	1.02	0.03	0.003	0.04	0.37
Bituminous 2, high-C	Black	27.65	26.94	0.59	0.002		NA

^a Not available.

ash would initially sorb all of the mercury vapor from the gas stream and would with each succeeding day saturate at a higher rate. This observation added a level of complexity to the determination of full loading for these samples.

3.2.5. Correlation of carbon content and mercury sorption

A comparison of values in the two columns in Table 4 showing mercury content with respect to carbon content reveals some interesting trends. If the amount of mercury per gram of carbon using preloading values is compared, it can be seen that the samples fall into distinct groups with similarities among separated fractions. This would indicate that mercury is evenly distributed in the carbon fraction or that during electrostatic separation there was a partitioning of mercury-containing fractions that correlated with the partitioning of carbon. It is more likely that the mercury was associated with the carbon, since the phenomenon was relatively reproducible between the sample types separated.

Postloading results are more difficult to interpret. It should be noted that, especially with the higher-carbon fractions, total loading was likely to be never achieved. The practice was to load mercury onto the sample until breakthrough and apparent saturation occurred. Samples were then allowed to sit overnight, and loading was repeated on the following day to ensure that equilibrium had been reached. Higher-carbon samples had a tendency to regenerate mercury-sorbing capacity upon aging overnight. Samples that had reached near-saturation would totally remove mercury from the gas stream at the beginning of each new day, and the high-carbon samples continued to do so for a week or more. This phenomenon, although interesting, made saturation a rather vague concept. More work is needed to fully understand the phenomenon of apparent regeneration. Several explanations are possible. Samples were sealed and isolated overnight; thus mercury loss is not likely. Mercury may have migrated into carbon granule interiors, thus exposing fresh carbon surfaces for sorption the following day. Alternately, if metallic constituents were present on carbon granules or on ash particles, mercury sorbed onto carbon may have migrated into reduced metals, again renewing the capacity of the carbon to sorb mercury. Determination of the mechanism of this phenomenon was beyond the scope of this project.

A statistical or graphic comparison of mercury concentrations before and after loading might have been interesting; however, laboratory loading was done using only mercury vapor and was also done at higher concentrations than would be found in a power generation station. Thus a comparison of preloading versus postloading mercury concentrations might be misleading. As additional data are generated and as experiments progress in this ongoing research effort, this comparison may be possible. During mercury-loading experiments, a sinusoidal wave appeared to be superimposed over the data recorded by the fluorescence detector monitoring output mercury concentration. The period of this wave was 10 min, which coincided

with a function of the air-handling system of the laboratory. Recording of ambient temperature indicated that a variation of laboratory temperature of between 3 and 5°F coincided with the variation of the output of the monitor. It was determined experimentally that the effect was on the sorptive capacity of the ash and not on other subcomponents of the system. The problem was reduced but not totally eliminated by placing the tube containing the ash in a water bath. This bath, which was not temperature controlled, acted as a moderator and remained at approximately average room temperature. The minor fluctuations in concentrations still noted were believed to be caused by a variation of input gas temperature and continued to coincide with the ambient temperature in the laboratory. This temperature dependence of uptake of mercury vapor as saturation of the ash occurred was somewhat unexpected, but interesting, and became an important consideration in the design of future experiments.

4. Conclusions and recommendations

The following conclusions can be drawn from the results presented:

- A direct correlation apparently exists between carbon content and mercury partitioning among individual ash samples.
- The direct relationship between carbon content and mercury-sorbing capacity of the bulk ash samples demonstrated in the loading experiments is not reflected by the information gathered on the low- and high-carbon fractions.
- The mercury-sorbing capacity of the inorganic fraction is extremely low with respect to carbon present in the ash; however, the amount of carbon remaining in the ash may not be a good indication of the capacity of the ash to capture mercury during the combustion and ash collection processes.
- Carbon appeared in several distinct forms in the ash. A strong possibility exists that there are significant differences between the mercury-sorbing capacities of these various carbon forms.
- The mercury-sorbing capacity of ash studied in this research was highly temperature dependent. A room temperature variation of only 3–5°F significantly affected the sorbing capacity of the ash as it was being loaded. Room temperature fluctuations were evident in the uptake curves of ash being loaded, making interpretation of uptake curves difficult. Thermostating the ash somewhat reduced this phenomenon.

References

- [1] Pavlish JH, Gerlach TR, Zygarlicke CJ, Pflughoeft-Hassett DF. Mitigation of air toxics from lignite generation facilities. Energy and Environmental Research Center Final Report, 1995.
- [2] Laudal DL, Galbreath KC, Heidt MK. A state-of-the-art review of flue gas mercury speciation methods. Electric Power Research Institute Report TR-107680 3471, 1996.